

Peer review status:

This is a non-peer-reviewed preprint submitted to EarthArXiv.

A Comparative Evaluation of Advanced Urban Data Methods in WRF

Jacobo Gabeiras¹, Chantal Staquet¹, Charles Chemel², Alberto Martilli³

¹Université Grenoble Alpes, CNRS, Grenoble INP, LEGI, France

²National Centre for Atmospheric Science, NCAS, Leeds, UK

³Centro de Investigaciones Energéticas, Medioambientales y Tecnológicas, CIEMAT, Spain

Email: jacobo.gabeiras@univ-grenoble-alpes.fr

Abstract.

Accurate representation of urban form is essential for simulating near-surface temperatures and the Urban Heat Island (UHI) effect in high-resolution mesoscale models. While WRF offers advanced urban parameterizations such as BEP+BEM, the realism of simulations remains strongly influenced by the input urban morphology data. This study compares the impact of three urban datasets—WUDAPT-based LCZs (via W2W), globally available high-resolution inputs integrated through the WRFUP Python package, and a detailed LiDAR-derived dataset—on WRF-BEP+BEM simulations of the August 2023 heatwave in Grenoble, France. Results show that WRFUP improves spatial accuracy and reduces nighttime warm biases relative to W2W, while LiDAR data achieves the best overall performance but with limited scalability. Despite improved inputs, persistent biases highlight the need for further advances in turbulence and surface energy modeling. These findings emphasize the importance of high-resolution urban data and provide a replicable framework for evaluating urban climate models.

1 Introduction

The Urban Heat Island (UHI) effect is characterized by higher temperatures in urban areas compared to their rural surroundings, enhancing heat stress, increasing energy demands, and creating a serious threat to public health, especially during heatwave events (Liao et al., 2018; Marcotullio et al., 2022). This is due to increased impervious surfaces, reduced vegetation, and complex urban morphologies, which alter the surface energy balance and atmospheric dynamics in urban areas (Ballinas & Barradas, 2016; Nardino & Laruccia, 2019). With cities expanding, and extreme heat events occurring more often as a consequence of climate change, there is a growing and urgent need to understand the drivers of urban heat to support the development of strategies for mitigating this UHI effect and increase urban resilience through sustainable urban planning (Barradas et al., 2022; Mutani & Todeschi, 2020).

The study of the response of city scale temperature distribution and UHI effects to such strategies needs a robust atmospheric model able to resolve fine-scale atmospheric processes and surface-atmosphere interactions (Bueno et al., 2012; Suter et al., 2022). The Weather Research and Forecast model (Skamarock et al., 2008, WRF) is one of the most applied tools in simulating the urban climate due to its capability for capturing the complex interactions between urban surfaces and atmospheric processes (Barlage et al., 2016; Martilli et al., 2024; Meyer et al., 2020). Accurate urban simulations with WRF depend on the urban parameterization such as the BEP (Martilli et al., 2002, Building Effect Parameterization) and BEM (Salamanca et al., 2010, Building Energy Model), which calculates how urban surfaces impact the surface energy balance and heat transport. These parameterizations strongly depend on the quality of the input fields that describe the city at each grid cell, including:

- Urban Fraction (UF) The fraction of each grid cell covered by construction.
- Plan Area Fraction (AF) The ratio of building footprint area to the grid cell area.
- Building Surface Fraction (SF) The fraction of total building surface.
- Mean Building Height (BH) The building height average weighted with AF.

There are a variety of different ways to derive these parameters, each representing some form of trade-off between accuracy, accessibility, and computational effort. The WUDAPT Local Climate Zone (LCZ) dataset (Ching et al., 2018) is one globally available, relatively simple approach to urban parameterization with the use of tools such as the LCZ generator (Demuzere et al., 2021). This method is enhanced with the use of WUDAPT To WRF (Demuzere et al., 2022, W2W), which facilitates the integration of LCZ-based urban morphology into WRF, while adding granularity through its clever approach. However, LCZ-based methods depend on a generalized urban classification and values that may potentially oversimplify urban morphology and thereby reduce UHI simulation accuracy (Stewart & Oke, 2012).

High-resolution data sources acquired through LiDAR technology are considered the most accurate option when available, as they represent urban structures in great detail, like building geometries and canopy elements (Münzinger et al., 2022; Wei & Yao, 2015). However, it is not universally available, and when it is, acquisition and preprocessing are labor-intensive, limiting the practical use of LiDAR for large-scale applications (Sailor, 2011).

To bridge the gap between simplicity and accuracy, the Python package WRFUP (Gabeiras, 2024, WRF Urban Parameters) leverages globally available datasets such as the World Settlement Footprint 3D (Esch et al., 2022, WSF3D) to compute urban parameters with higher spatial accuracy than LCZ-based approaches, while maintaining ease of implementation. Beyond improving spatial resolution, WRFUP also provides access to continuously updated, state-of-theart global datasets, ensuring that users can incorporate the latest urban morphology data into their simulations. This is particularly relevant given the challenges of updating static datasets within WRF, or changing the study domain, which often requires manual data migration and adaptation. Furthermore, certain urban parameters require field-specific calculations such as the weighted mean of the building heights based on the plan area fraction. By automating the integration of these evolving datasets, WRFUP serves as a promising alternative that balances realism with computational practicality. This study examines how WRFUP compares to existing approaches by evaluating its efficiency and accuracy relative to W2W and LiDAR-based datasets, providing insights into its applicability for urban climate modeling.

To this end, it examines the performance of the three methods in simulating near-surface temperature, and urban heat island intensity (UHII) during the severe heatwave in Grenoble, France, from August 19 to 23, 2023. This extreme event, which amplified the UHI effect to 6°C, serves as an ideal test case, as it highlights the challenges of accurately modeling urban heat dynamics

The paper is structured as follows: Section 2 presents the study area, while Section 3 details the WRF model setup, urban parameterization, and validation methods. Section 4.1 compares urban parameters, and Section 4.2 analyzes temperature results using LiDAR as a reference. Sections 4.3 and 4.4 validate near-surface temperature and UHI with observations. Section 5 examines trade-offs between accuracy, complexity, and practicality, and Section 6 provides conclusions and future directions.

2 Study Area

The Grenoble Metropolitan Area is located in southeastern France, deeply set inside an alpine valley sheltered by mountain ranges Chartreuse, Vercors, and Belledonne. The steep terrain, intense urbanization and construction materials makes Grenoble particularly prone to the UHI effect because of the poor ventilation and trapping of heat that take place, particularly during heatwaves (Foissard et al., 2024). The metropolitan area, consisting of 49 municipalities, with approximately 450,000 inhabitants, saw rapid growth throughout the 20th century; causing much of its building stock to be made with poorly insulated materials. These materials contribute much to outdoor and indoor heat retention and cooling demand and increased energy during hot periods.

3 Methods and Data

3.1 WRF Model Setup

The WRF model was used to simulate the heatwave event of 19 to 23 August 2023. The 19th was used for spin up time, and the results here correspond to the four days from the 20th to the 23rd included. The configuration uses one-way-nesting with the outer domain D01 with 9 km grid cell size, an intermediate domain D02 covering central Europe and the Mediterranean at 1 km, and the innermost domain, D03, covering a resolution of 200 m. Figure 1 shows all domains centered over Grenoble Metropolitan Area. The urban parameterization used is the latest version of BEP+BEM+COMFORT (Martilli et al., 2024). The Bougeault and Lacarrère planetary boundary layer (PBL) scheme (Bougeault & Lacarrere, 1989) was used to simulate vertical mixing and turbulence.

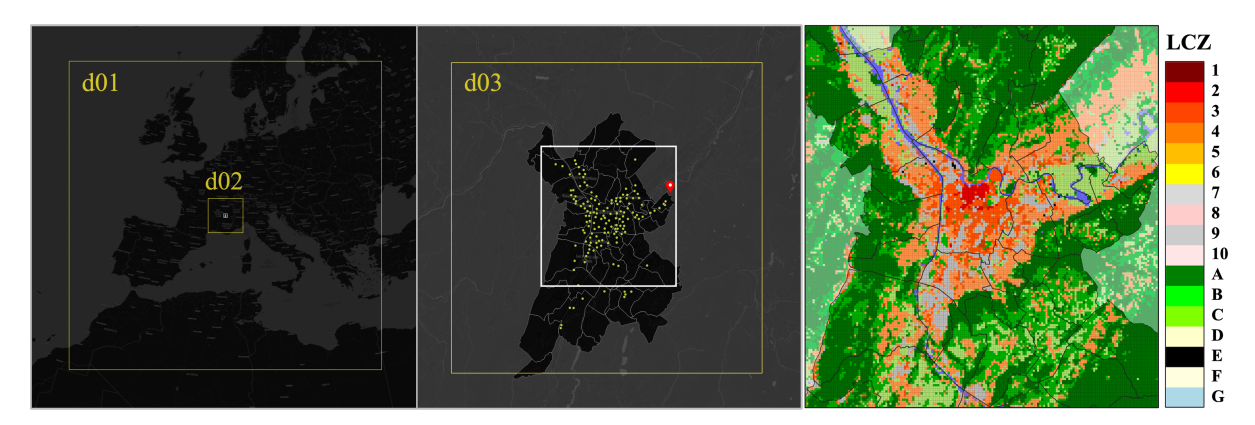


Figure 1: Overview of the WRF nested domains and the LCZ classification for the Grenoble Metropolitan Area. Left: The outer domain (d01) spans a large portion of Europe, and the intermediate domain (d02) focuses on southeastern France. Center: The innermost domain (d03) provides high-resolution coverage of Grenoble and its surroundings; yellow dots denote the temperature sensor locations, and the red marker indicates the Meteo France station used as a rural reference for UHI calculations. The white square highlights the area where over 95% of the population resides. Right: LCZ classification within the white squared area, showing the distribution of built-up zones.

3.2 Input Data and Simulations Performed

The three methods (W2W, WRFUP, and LiDAR) rely on different data sources, resolution, coverage, and level of detail, affecting their suitability for urban climate applications.

W2W uses the WUDAPT LCZ dataset (Ching et al., 2018), which classifies urban areas into broad categories based on Landsat imagery and crowd-sourced training data. This globally available dataset provides a straightforward approach to urban parameterization. To estimate urban parameters, W2W assigns each LCZ the median values from the LCZ classification table of Stewart and Oke (2012) and applies a spatial averaging process on the model grid. This approach enhances granularity by smoothing abrupt transitions between urban classes. While well-suited for coarser-resolution applications or regions with limited urban data, its discrete classification scheme limits the representation of urban morphological variability at high resolutions.

WRFUP derives urban parameters following the method described in the WRFUP technical documentation (Gabeiras, 2024) from three globally available datasets. The World Settlement Footprint 3D (Esch et al., 2022, WSF3D, 90 m) provides building footprint fractions and building height data, forming the foundation for urban fraction calculations. The Global Urban Fraction dataset Patel and Roth, 2022, pp. 100 m refines urban fraction estimates by offering an independent, high-resolution representation of urbanized areas. Additionally, WRFUP includes a custom global dataset for building surface fraction (Gabeiras, 2025), calculated in accordance with the methodology of the model BEP.

LiDAR-based methods rely on airborne or terrestrial LiDAR surveys, such as those provided by national mapping agencies (IGN, 2023, IGN LIDAR HD for France). These datasets offer the highest spatial resolution, capturing detailed building geometries for precise calculation of building heights, plan area fraction, and building surface fraction. While considered the gold standard for urban morphology, LiDAR data is computationally demanding and often limited to specific regions, restricting its use in large-scale applications. LiDAR point clouds contain millions of elevation points that require processing to extract urban morphology parameters. The raw data is filtered and classified to distinguish buildings from ground and vegetation. This product was cross-referenced with the Microsoft Building Footprints dataset (Microsoft AI for Good Team, 2023), which provides extensive building outlines. The urban parameters were derived and rasterized onto the model grid following the National Urban Data and Access Portal Tool (NUDAPT) guidelines (Glotfelty et al., 2013).

To evaluate the influence of the different urban parameterization methods on model performance, three simulations were conducted, each using a different method: S1 (W2W,WUDAPT/LCZ-based), S2 (prepared with WRFUP), and S3 (LiDAR-derived urban parameters). Table 1 summarizes the key features of the datasets used in these simulations, highlighting the trade-offs between accuracy, coverage, and ease of implementation.

All simulations were forced with ERA5 hourly data (C3S, 2018a, 2018b), and use the same land cover description, with urban areas represented through Local Climate Zones (LCZs). The LCZ classification was obtained using the LCZ Generator from the WUDAPT project, ensuring consistency across all simulations. In the model grid, the resulting LCZ map appears as shown in Figure 1.

Table 1: Overview of the three simulations, their urban parameterization methods, and data sources.

Sim.	Method	Data Sources	Resolution	Coverage
S1	W2W	WUDAPT LCZ	100 m	Global
S2	WRFUP	WSF3D, Urban Fraction, UrbanSurfAce	90-100 m	Global
S3	LiDAR	IGN LIDAR, Microsoft Buildings	Sub-meter	Regional

3.3 Validation Data and Method

The performance of the urban parameterization methods is evaluated using data from a high-density temperature measurement network deployed across Grenoble, Echirolles, and other communes within the Grenoble Métropole. Established in 2019, this network consists of 144 sensors, including 62 within Grenoble and Echirolles, mounted on 3-meter-high streetlights. The sensor locations were selected based on a preliminary classification of neighborhood typologies using the Local Climate Zone system, ensuring comprehensive coverage of urban, peri-urban, and rural areas. This extensive dataset captures detailed spatial and temporal variations in near-surface temperature and UHII, providing a robust foundation for validating the urban parameterization methods.

To evaluate the impact of urban parameterization on near-surface temperature and UHI simulation, we conduct a systematic comparison of three methods: W2W, WRFUP, and LiDAR-derived urban parameters. First, we assess how well W2W and WRFUP reproduce key urban parameters—urban fraction, plan area fraction, surface fraction, and building height—compared to LiDAR, using spatial maps and statistical analyses. Next, we examine the influence of these parameterization methods on simulated near-surface temperature (3 m), validating results against LiDAR-based estimates. To further assess model accuracy, we compare the simulated near-surface temperature from all three methods with observational data from Grenoble's high-density meteorological network, evaluating temperature bias and correlation. Finally, we analyze the UHI effect, comparing average UHII maps across methods and assessing their agreement with previous UHI studies in Grenoble and station-based UHII observations.

4 Results

4.1 Urban Parameter Comparison

This section evaluates the urban parameters derived from W2W and WRFUP on the model grid, comparing them against LiDAR-based data, which serves as the reference due to its high spatial resolution. The comparison focuses on the four key parameters introduced previously: urban fraction (UF), plan area fraction (AF), surface fraction (SF), and building height (BH).

Figure 2 presents spatial maps obtained at the model grid, of these parameters across Grenoble for each method. The W2W-derived parameters appear coarser, reflecting the categorical nature of the WUDAPT LCZ dataset, which generalizes urban morphology into predefined zones. In contrast, WRFUP shows finer spatial variations, capturing more localized differences in urban density and building structures due to its reliance on high-resolution datasets. Compared to LiDAR, WRFUP exhibits greater detail, while W2W tends to produce homogeneous fields within each LCZ and abrupt changes in between LCZs.

To quantify the agreement between methods, Figure 3 presents scatter plots and Kernel Density Estimations (KDEs) comparing W2W and WRFUP against LiDAR for each parameter. WRFUP consistently shows higher correlation coefficients (R^2) with LiDAR than W2W, particularly for urban fraction ($R^2 = 0.58$ vs. $R^2 = 0.37$) and building height ($R^2 = 0.29$ vs. $R^2 = 0.12$). The KDE plots further highlight that WRFUP distributions closely match those of LiDAR, while W2W exhibits larger deviations and broader spreads.

Overall, these results indicate that WRFUP provides a significant improvement over W2W in capturing urban morphology, reducing errors associated with LCZ-based parameterization. This improved accuracy is expected to enhance near-surface temperature simulations, which will be assessed in the following section.

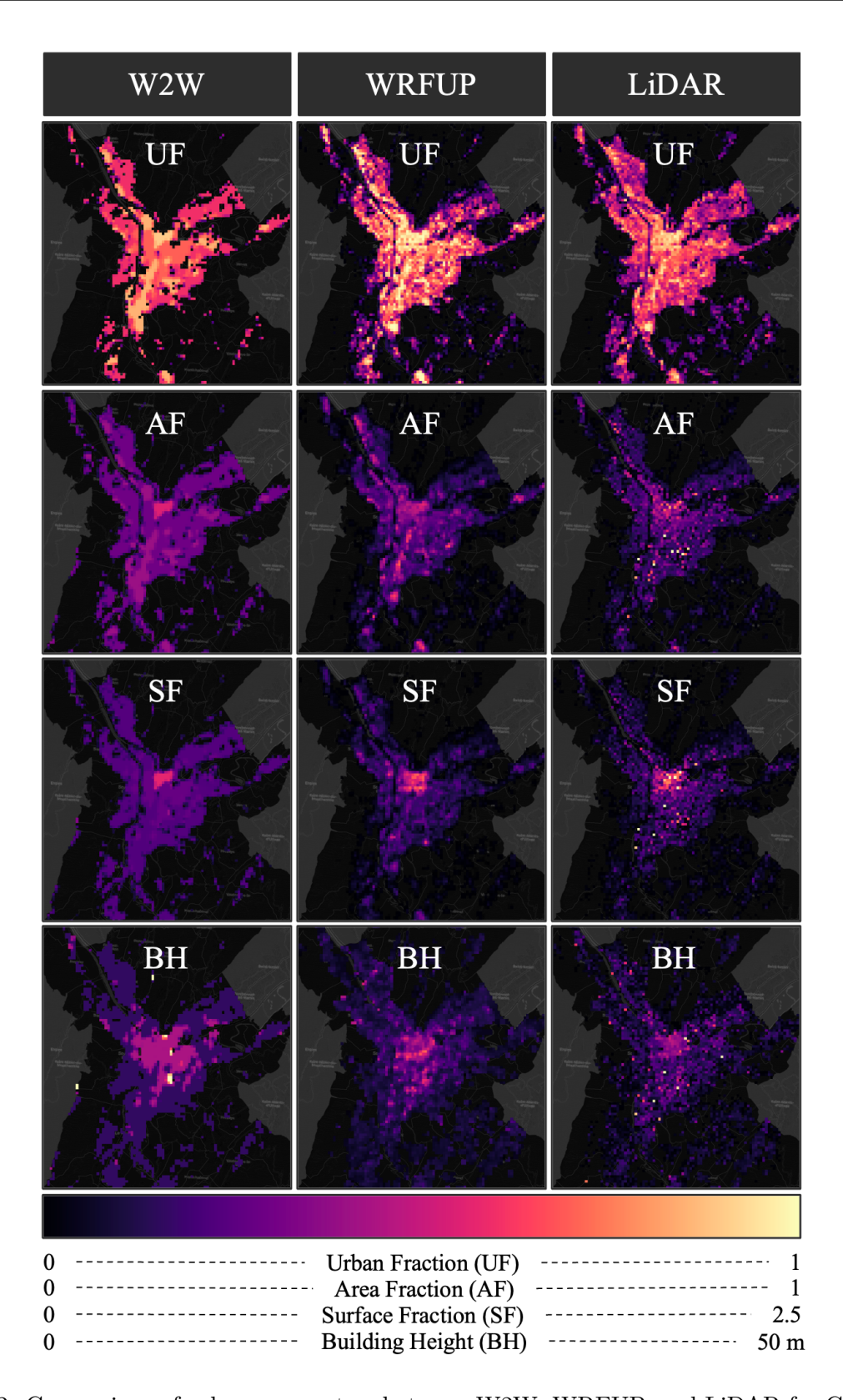


Figure 2: Comparison of urban parameters between W2W, WRFUP, and LiDAR for Grenoble. Rows represent different parameters: urban fraction (UF), plan area fraction (AF), surface fraction (SF), and building height (BH).

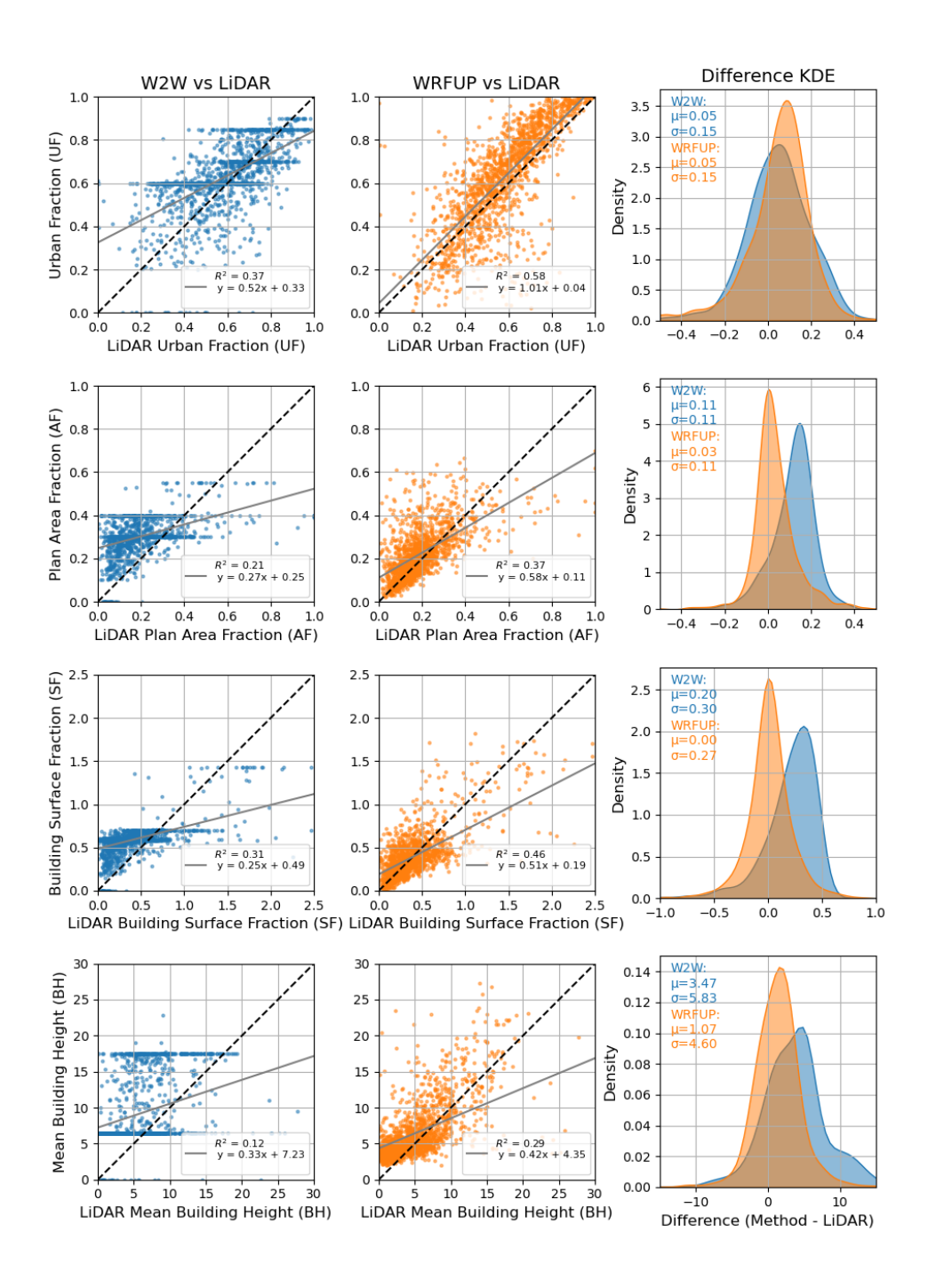


Figure 3: Statistical comparison of urban parameters derived from W2W and WRFUP against LiDAR. Left: Scatter plots showing correlation for each parameter. Right: Kernel Density Estimation (KDE) plots highlighting the distribution differences.

4.2 Temperature Results With Lidar As Reference

Since LiDAR provides the most detailed and accurate representation of urban morphology available, it is expected to yield the most physically realistic temperature simulation. For this reason, S3 serves as a reference benchmark to evaluate how well S1 and S2 (W2W and WRFUP-based methods) capture near-surface heat dynamics. This comparison allows us to assess the impact of urban parameter differences before considering observational validation in later sections.

Figure 4 presents the KDE distributions of temperature differences for S1 and S2 relative to S3. The mean temperature difference between S1 and S3 is -0.39° C, with a standard deviation of 0.58° C, whereas S2 shows a lower mean bias of -0.14° C and a standard deviation of 0.48° C. These results indicate that S2 exhibits lower systematic biases in temperature predictions relative to LiDAR and a reduced spread, suggesting that its urban parameterization better aligns with the morphology captured in LiDAR-based simulations.

The differences between S1 and S2 are not uniform throughout the day. The bias is smaller during the daytime and becomes more pronounced at night, when S1 shows a positive mean difference of +0.5°C, while S2 exhibits a smaller negative bias of -0.25°C. This pattern suggests that S1 retains more heat at night, while S2 loses heat slightly quicker compared to the results with LiDAR. This behavior can be linked to differences in the urban parameters. S1 overestimates all four parameters (Figure 3), leading to an exaggerated heat storage effect during the day, which then results in higher nighttime temperatures compared to LiDAR. In contrast, S2 although still slightly overestimates these parameters, it aligns more closely with LiDAR values. However it still shows a slight tendency to cool down below S3.

The difference in bias dispersion between day and night is also notable. This is possibly due to the following mechanism. During the day, solar radiation dominates surface energy fluxes, and convective mixing within the boundary layer reduces spatial inconsistencies in temperature. As a result, biases are relatively smaller and less dispersed. At night, surface cooling depends more directly on urban morphology, and the shallow, stable nocturnal boundary layer amplifies local variations in heat retention. This leads to greater spread in temperature differences, particularly for S1. S2 consistently shows less dispersion than S1, especially during the day.

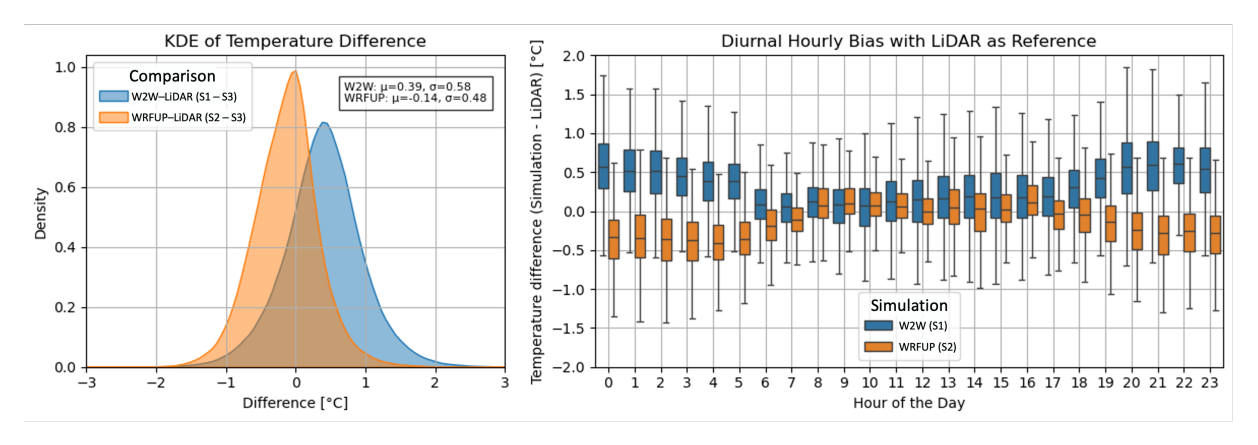


Figure 4: Comparison of simulated near-surface temperature (3 m) differences relative to LiDAR-based simulation. The results correspond to the four days from the 20th to the 23rd included, August 2023.

These findings show that WRFUP produces near-surface temperature simulations that are generally closer to those obtained with LiDAR-based urban morphology than W2W. However, this comparison alone does not indicate how either method performs relative to real-world temperature observations. The next section will further analyze these differences by comparing both methods against high-density observational data.

4.3 Validation Against Observed Near-Surface Temperatures

To evaluate the accuracy of W2W, WRFUP, and LiDAR-based simulations, we compare their near-surface temperature (3 m) outputs against high-density meteorological station observations across Grenoble Metropolitan Area.

Figure 5 shows the diurnal cycle of bias (simulated minus observed). All three simulations consistently overestimate nighttime temperatures and underestimate daytime ones. The night-time bias is largest for S1, exceeding $+2^{\circ}$ C, while S2 and S3 reduce this overestimation. During the daytime, all methods underestimate temperature, with the strongest bias occurring in the late afternoon.

The correlation coefficients (R values) indicate that all methods reproduce nighttime temperatures better than daytime ones. For daily minimum temperatures, S2 (R=0.74) and S3 (R=0.75) show stronger agreement with observations than S1 (R=0.67). However, for daily maximum temperatures, all models perform significantly worse, with S2 (R=0.21) showing the lowest correlation, followed by S3 (R=0.28) and S1 (R=0.35). Although S1 performed better in this case, all methods struggle to reproduce daytime peak temperatures, likely due to deficiencies beyond urban morphology alone.

These results confirm that differences in urban parameterization impact model accuracy, particularly at night. However, all methods struggle with daytime underestimation, suggesting a model's inability beyond urban morphology data.

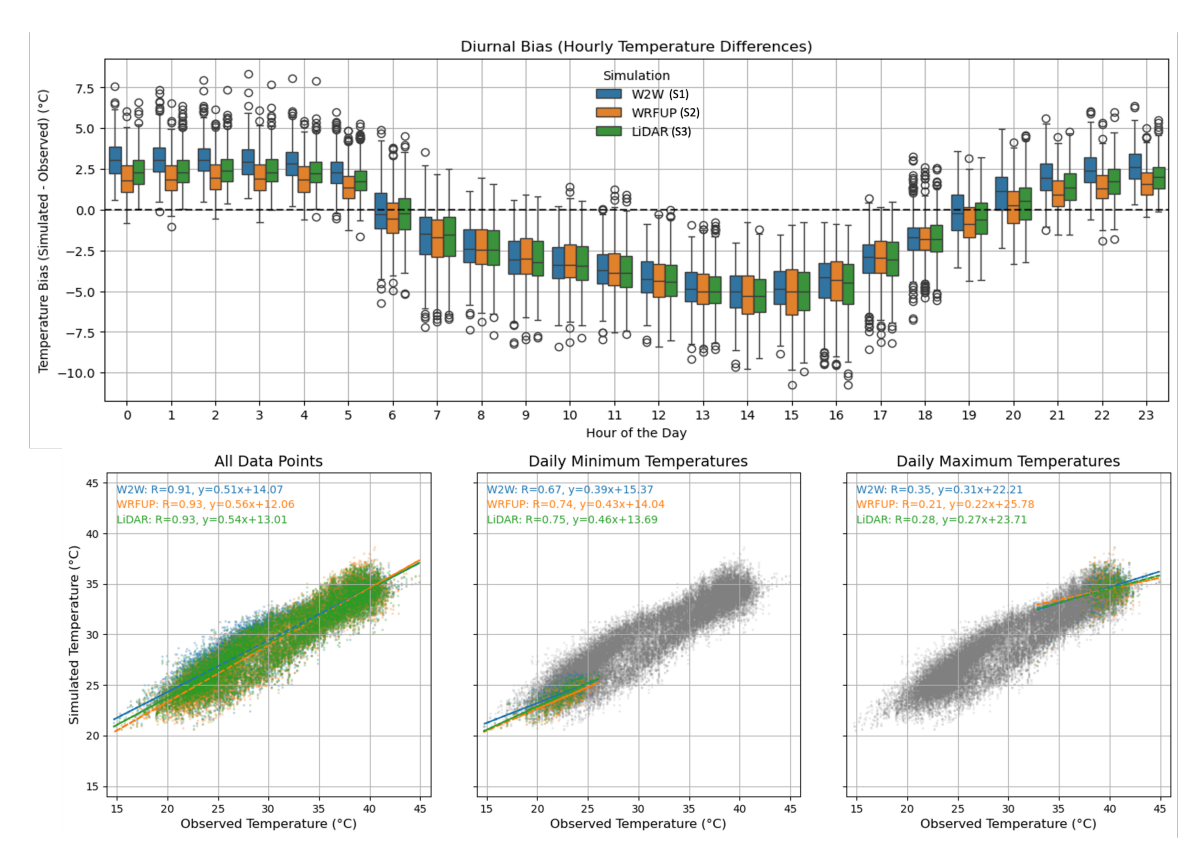


Figure 5: Comparison of simulated and observed near-surface temperatures (3 m). Top: diurnal cycle of temperature bias (simulated minus observed). Bottom: scatter plots of simulated vs. observed temperatures, including all data points, daily minimum temperatures, and daily maximum temperatures. The results correspond to the four days from the 20th to the 23rd included, August 2023.

4.4 Urban Heat Island Intensity Estimation

A key motivation for the use of urban climate models is the ability to quantify and analyze the Urban Heat Island effect, both in terms of its intensity and spatial structure. In this section, we evaluate how the different methods influence the simulated Urban Heat Island Intensity (UHII). UHII is defined as the difference between the daily minimum temperature at a given location and the daily minimum temperature at the reference rural station:

$$UHII(x,y) = T_{\min}(x,y) - T_{\min}^{\text{rural}}$$
(1)

where $T_{\min}(x,y)$ is the daily minimum temperature at a specific grid cell (x,y), and T_{\min}^{rural} is the daily minimum temperature recorded at the rural reference station, in this case Le Versoud airport station, marked in red in Figure 1. The maps in Figure 7 represent the average UHII over the four nights of the heatwave compared to a previous study of the UHII performed over the same heatwave with the use of a geostatistical model by Xavier Foissard (AURG, 2022).

All simulations capture the overall structure of the UHII, with the strongest warming concentrated in central Grenoble. However, key differences emerge in how UHII is spatially distributed. S1 exhibits a more uniform UHI structure that closely follows the map of Local Climate Zone (LCZ) classification (see Figure 1), as its urban parameterization relies on LCZ definitions. The main hotspot in W2W's simulation aligns with LCZ 2, corresponding to compact mid-rise urban areas. However, when comparing to the independent UHI study by Xavier Foissard (AURG, 2022) (bottom-right panel of Figure 7), it becomes evident that the actual hotspot extends beyond the area classified as LCZ 2 in S1.

WRFUP and LiDAR-based simulations better capture this extended hotspot as they rely directly on urban morphology data rather than pre-defined LCZ categories. By incorporating high-resolution data, these methods provide a spatial distribution of UHII that better resembles the one obtained through a geostatistical model (Foissard & Fouvet, 2022).

To quantify these differences, Figure 6 presents the correlation between simulated UHII and observed data, as well as the mean absolute error (MAE) per night. Across all nights, S2 consistently outperforms S1, achieving higher correlation and lower MAE. S3 remains the best-performing simulation, and S2 shows a improvement over S1.

These findings highlight that higher spatial detail in urban morphology enhances UHII representation. WRFUP, by integrating high-resolution global datasets, significantly improves spatial accuracy compared to W2W while remaining computationally efficient.

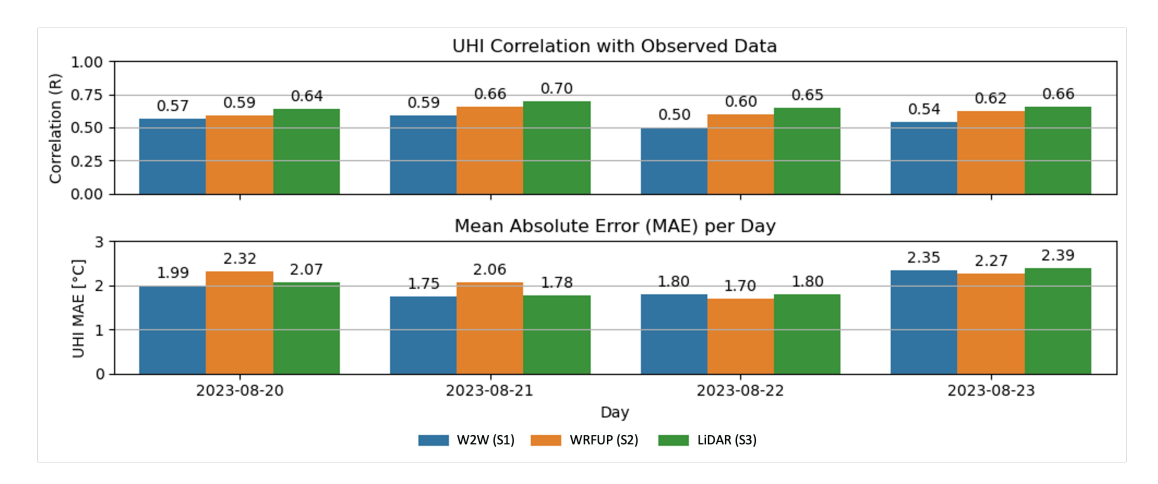


Figure 6: Top: Correlation of simulated UHII with observed data for each night of the simulated period. Bottom: Mean Absolute Error (MAE) per day.

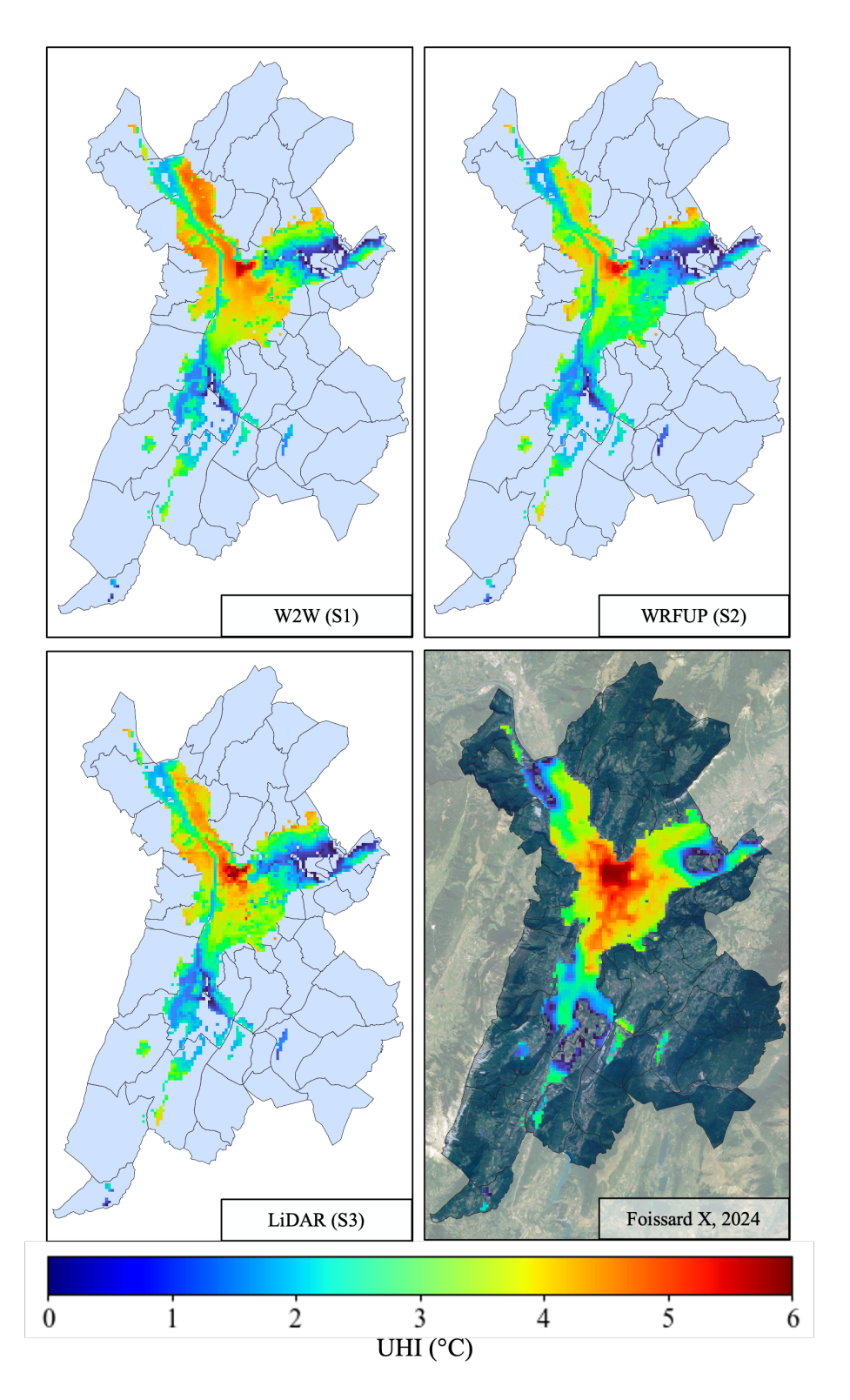


Figure 7: Urban Heat Island Intensity (UHII) maps, computed as the difference between the daily minimum temperature at each point and the daily minimum temperature at the Le Versoud station. The maps show the average UHII over four nights from the 20th to the 23rd of August 2023 included. The bottom-right panel represents the UHI study by Foissard (AURG, 2022) for the same heatwave and is included for qualitative comparison.

5 Discussion

The results of this study demonstrate the strong influence of urban parameterization methods on near-surface temperature and UHI simulations. Among the three approaches, the LiDAR-based method serves as the most detailed and physically realistic reference. However, its computational demands and limited availability make it impractical for large-scale applications, emphasizing the need for alternatives that balance accuracy and accessibility.

WRFUP emerges as a promising solution, offering significantly improved accuracy over W2W while maintaining global availability and practicality. Unlike W2W, which assigns fixed LCZ categories to grid cells, WRFUP derives urban parameters from high-resolution datasets, producing a more detailed spatial representation of urban morphology that closely resembles LiDAR products while maintaining an ease of use similar to that of W2W. This improvement results in lower temperature biases and a more accurate distribution of UHI intensity, aligning more closely with the LiDAR-based simulation.

W2W, despite its limitations, remains a clever and valuable approach, particularly for coarser-resolution simulations where categorical classification helps simplify urban representation and its utility for ingesting the LCZ products as land use cover into WRF Preprocessing System (WPS) files. However, at high resolutions (such as the 200 m grid used here), its rigid LCZ framework introduces abrupt spatial transitions that limit accuracy. This study, therefore, serves as a test case for high-resolution urban climate modeling, where WRFUP provides a meaningful step forward.

Despite these improvements, all methods exhibit systematic biases, particularly an underestimation of daytime temperatures, suggesting that urban morphology alone does not fully explain temperature discrepancies. Nighttime temperature overestimation, prominent in W2W simulation, is notably reduced with WRFUP, reinforcing the role of improved urban representation in heat retention estimates. However, the fact that strong biases persist even with high-resolution urban data such as LiDAR suggests that model physics itself requires further refinement. This highlights the need for improvements beyond urban morphology, particularly in surface energy balance processes.

These findings highlight the importance of detailed urban morphology in urban climate modeling, challenging studies that downplay its influence. Often, model improvements are difficult to detect due to limited observational coverage, but the high-density station network used in this study allows for a more precise assessment. The results suggest that better urban parameterization does improve simulations when validated with sufficient observational data, yet also underline the need for broader advancements in model physics. In simple terms, while improving urban input data is important, it is not sufficient by itself to fully resolve the simulation biases.

A key limitation of this study is its focus on a single heatwave in Grenoble. Further testing across different cities and climate conditions is needed to fully assess WRFUP's robustness. Future research should explore hybrid approaches that integrate WRFUP with additional globally available data to further enhance model accuracy.

6 Conclusion

This study compared three urban parameterization methods—W2W, WRFUP, and LiDAR-based parameterization—in their ability to simulate near-surface temperature and urban heat island (UHI) intensity during the August 19–23, 2023 heatwave in Grenoble, France. The results show that urban parameterization significantly affects model performance, particularly in nighttime temperature and UHI representation.

WRFUP emerges as a promising alternative to both W2W and LiDAR, offering a balance

between accuracy and computational efficiency. Unlike W2W, which relies on LCZ classifications, WRFUP computes continuous urban parameters from high-resolution, globally available datasets, resulting in a more realistic representation of urban morphology. Compared to the LiDAR-based approach, WRFUP produces similar spatial distributions of urban parameters and temperatures while avoiding the data-intensive requirements of LiDAR processing.

In addition to evaluating urban parameterization methods, this study also produced a high-resolution LiDAR-derived building dataset for Grenoble, providing a valuable benchmark for local urban morphology representation. This dataset can serve as a valuable reference for future research in the local urban climate modeling, adaptation planning, and other applications requiring accurate building data.

Despite these improvements, all methods exhibit a tendency to underestimate daytime temperatures, highlighting the need for further refinement of urban surface energy fluxes in WRF simulations. The findings underscore the importance of accurate urban parameterization for urban climate modeling and suggest that integrating high-resolution building and land cover datasets can lead to more reliable simulations. However, the persistence of biases even with high-resolution data highlights the need for further improvements in urban climate modeling beyond morphology alone, particularly in surface energy balance representation.

Future work should focus on testing WRFUP in different urban environments and evaluating its performance across a range of climate conditions. Further refinement of urban surface processes, including anthropogenic heat flux and radiative transfer models, could help reduce remaining biases in temperature simulations. By improving the representation of urban morphology, WRFUP offers a valuable tool for enhancing urban climate modeling and supporting climate adaptation strategies in cities worldwide.

References

- AURG. (2022). La Métropole cartographie ses îlots de chaleur urbains. https://www.aurg.fr/article/442/2205-la-metropole-cartographie-ses-ilots-de-chaleur-urbains.htm
 Accessed: 2025-02-06.
- Ballinas, M., & Barradas, V. L. (2016). The Urban Tree as a Tool to Mitigate the Urban Heat Island in Mexico City: A Simple Phenomenological Model. *Journal of Environmental Quality*, 45(1), 157–166. https://doi.org/10.2134/jeq2015.01.0056
- Barlage, M., Miao, S., & Chen, F. (2016). Impact of physics parameterizations on high-resolution weather prediction over two Chinese megacities. *Journal of Geophysical Research: Atmospheres*, 121(9), 4487–4498. https://doi.org/10.1002/2015jd024450
- Barradas, V. L., Miranda, J. A., Esperón-Rodríguez, M., & Ballinas, M. (2022). (Re)Designing Urban Parks to Maximize Urban Heat Island Mitigation by Natural Means. *Forests*, 13(7), 1143. https://doi.org/10.3390/f13071143
- Bougeault, P., & Lacarrere, P. (1989). Parameterization of Orography-Induced Turbulence in a Mesobeta–Scale Model. *Monthly Weather Review*, 117(8), 1872–1890. https://doi.org/10.1175/1520-0493(1989)117<1872:POOITI>2.0.CO;2
- Bueno, B., Pigeon, G., Norford, L. K., Zibouche, K., & Marchadier, C. (2012). Development and evaluation of a building energy model integrated in the TEB scheme. *Geoscientific Model Development*, 5(2), 433–448. https://doi.org/10.5194/gmd-5-433-2012
- C3S. (2018a). ERA5 hourly data on pressure levels from 1940 to present. https://doi.org/10. 24381/CDS.BD0915C6
- C3S. (2018b). ERA5 hourly data on single levels from 1940 to present. https://doi.org/10.24381/CDS.ADBB2D47

- Ching, J., Mills, G., Bechtel, B., See, L., Feddema, J., Wang, X., Ren, C., Brousse, O., Martilli, A., Neophytou, M., Mouzourides, P., Stewart, I., Hanna, A., Ng, E., Foley, M., Alexander, P., Aliaga, D., Niyogi, D., Shreevastava, A., ... Theeuwes, N. (2018). WU-DAPT: An Urban Weather, Climate, and Environmental Modeling Infrastructure for the Anthropocene. Bulletin of the American Meteorological Society, 99(9), 1907–1924. https://doi.org/10.1175/bams-d-16-0236.1
- Demuzere, M., Argüeso, D., Zonato, A., & Kittner, J. (2022). W2W: A Python package that injects WUDAPT's Local Climate Zone information in WRF. *Journal of Open Source Software*, 7(76), 4432. https://doi.org/10.21105/joss.04432
- Demuzere, M., Kittner, J., & Bechtel, B. (2021). LCZ Generator: A Web Application to Create Local Climate Zone Maps. Frontiers in Environmental Science, 9, 637455. https://doi.org/10.3389/fenvs.2021.637455
- Esch, T., Brzoska, E., Dech, S., Leutner, B., Palacios-Lopez, D., Metz-Marconcini, A., Marconcini, M., Roth, A., & Zeidler, J. (2022). World Settlement Footprint 3D A first three-dimensional survey of the global building stock. Remote Sensing of Environment, 270, 112877. https://doi.org/10.1016/j.rse.2021.112877
- Foissard, X., & Fouvet, A.-C. (2022, November). L'îlot de chaleur urbain grenoblois (tech. rep.).
- Foissard, X., Masson, V., Hidalgo, J., Pigeon, G., & Schoetter, R. (2024). High spatial density temperature dataset for the Grenoble alpine valley: A tool for urban heat island investigation and climate services (tech. rep.) (Publication Title: Urban Climate Volume: 52). https://doi.org/10.1016/j.uclim.2024.102147
- Gabeiras, J. (2024). Wrfup: A Python package for urban parameter ingestion in WRF. https://github.com/jacobogabeiraspenas/wrfup
 Accessed: 2024-05-15.
- Gabeiras, J. (2025). UrbanData01: High-resolution urban datasets for WRFUP package. https://github.com/jacobogabeiraspenas/UrbanData01
 Accessed: 2025-02-06.
- Glotfelty, T., Tewari, M., Sampson, K., Duda, M., Chen, F., & Ching, J. (2013). National urban data and access portal tool documentation [Accessed: 2025-03-27].
- IGN. (2023). LiDAR HD High-Resolution Airborne LiDAR Data. https://geoservices.ign.fr/lidarhd Accessed: 2025-02-06.
- Liao, W., Liu, X., Li, D., Luo, M., Wang, D., Wang, S., Baldwin, J., Lin, L., Li, X., Feng, K., Hubacek, K., & Yang, X. (2018). Stronger Contributions of Urbanization to Heat Wave Trends in Wet Climates. *Geophysical Research Letters*, 45(20). https://doi.org/10.1029/2018GL079679
- Marcotullio, P. J., Keßler, C., & Fekete, B. M. (2022). Global urban exposure projections to extreme heatwaves. Frontiers in Built Environment, 8, 947496. https://doi.org/10.3389/fbuil.2022.947496
- Martilli, A., Clappier, A., & Rotach, M. W. (2002). An Urban Surface Exchange Parameterisation for Mesoscale Models. *Boundary-Layer Meteorology*, 104(2), 261–304. https://doi.org/10.1023/A:1016099921195
- Martilli, A., Nazarian, N., Krayenhoff, E. S., Lachapelle, J., Lu, J., Rivas, E., Rodriguez-Sanchez, A., Sanchez, B., & Santiago, J. L. (2024). WRF-Comfort: Simulating microscale variability in outdoor heat stress at the city scale with a mesoscale model. *Geoscientific Model Development*, 17(12), 5023–5039. https://doi.org/10.5194/gmd-17-5023-2024
- Meyer, D., Schoetter, R., Riechert, M., Verrelle, A., Tewari, M., Dudhia, J., Masson, V., van Reeuwijk, M., & Grimmond, S. (2020). WRF-TEB: Implementation and Evaluation of the Coupled Weather Research and Forecasting (WRF) and Town Energy Balance (TEB)

- Model. Journal of Advances in Modeling Earth Systems, 12(8). https://doi.org/10.1029/2019ms001961
- Microsoft AI for Good Team. (2023). Global ML Building Footprints. https://github.com/microsoft/GlobalMLBuildingFootprints
 Accessed: 2025-02-06.
- Münzinger, M., Prechtel, N., & Behnisch, M. (2022). Mapping the urban forest in detail: From LiDAR point clouds to 3D tree models. *Urban Forestry & Urban Greening*, 74, 127637. https://doi.org/10.1016/j.ufug.2022.127637
- Mutani, G., & Todeschi, V. (2020). Building energy modeling at neighborhood scale. *Energy Efficiency*, 13(7), 1353–1386. https://doi.org/10.1007/s12053-020-09882-4
- Nardino, M., & Laruccia, N. (2019). Land Use Changes in a Peri-Urban Area and Consequences on the Urban Heat Island. *Climate*, 7(11), 133. https://doi.org/10.3390/cli7110133
- Patel, P., & Roth, M. (2022, August). A High-Resolution Dataset of Global Urban Fraction for Mesoscale Urban Modelling. https://doi.org/10.5281/ZENODO.6994974
- Sailor, D. J. (2011). A review of methods for estimating anthropogenic heat and moisture emissions in the urban environment. *International Journal of Climatology*, 31(2), 189–199. https://doi.org/10.1002/joc.2106
- Salamanca, F., Krpo, A., Martilli, A., & Clappier, A. (2010). A new building energy model coupled with an urban canopy parameterization for urban climate simulations—part I. formulation, verification, and sensitivity analysis of the model. *Theoretical and Applied Climatology*, 99(3-4), 331–344. https://doi.org/10.1007/s00704-009-0142-9
- Skamarock, W., Klemp, J., Dudhia, J., Gill, D., Barker, D., Wang, W., Huang, X.-Y., & Duda, M. (2008). A Description of the Advanced Research WRF Version 3 (tech. rep.). UCAR/N-CAR. https://doi.org/10.5065/D68S4MVH
- Stewart, I. D., & Oke, T. R. (2012). Local Climate Zones for Urban Temperature Studies. Bulletin of the American Meteorological Society, 93(12), 1879–1900. https://doi.org/10.1175/bams-d-11-00019.1
- Suter, I., Grylls, T., Sützl, B. S., Owens, S. O., Wilson, C. E., & van Reeuwijk, M. (2022). uDALES 1.0: A large-eddy simulation model for urban environments. *Geoscientific Model Development*, 15(13), 5309–5335. https://doi.org/10.5194/gmd-15-5309-2022
- Wei, X., & Yao, X. (2015). 3d model construction in an urban environment from sparse lidar points and aerial photos a statistical approach. *Geometrica*, 69(3), 271–284. https://doi.org/10.5623/cig2015-302